JMEPEG (2005) 14:315-321
DOI: 10.1361/10599490523319

1059-9495/$19.00

Partitioning of Energy Loss in Glass-Fiber-Reinforced Polymers Under Transverse Loading

T. Kuboki, P-Y.B. Jar, and J.J.R. Cheng

(Submitted October 20, 2004; in revised form December 22, 2004)

Energy loss for (a) contact indentation and (b) friction between delaminating surfaces was measured experimentally to determine the energy required for matrix cracking and delamination in a glass-fiber-reinforced polymer (GFRP) under several levels of out-of-plane (transverse) quasistatic loading without fiber fracture. The results suggest that the friction between delaminating surfaces and the contact indentation contributed to 30% of the total energy loss. The delamination and matrix cracking were responsible for the remaining 70% of the total energy loss. Due to the significant portion of the total energy loss for the mechanisms unrelated to delamination, we conclude that correcting the measured energy loss is necessary to accurately quantify the GFRPs' delamination resistance.

Keywords failure analysis, mechanical testing, polymer matrix composites

1. Introduction

Fiber-reinforced polymers (FRP) are known to be vulnerable to loading in the direction perpendicular to the laminate surface (referred to as transverse loading hereafter), which has long been a major concern for their structural applications. The possible damage modes introduced by the transverse loading are matrix cracking, delamination, contact indentation, and fiber breakage (Ref 1-3), most of which can be generated unexpectedly during manufacturing, operation, or maintenance. Among these damage modes, delamination is known to be most dangerous, as it can lead to unexpected catastrophic failure of structures. Therefore, characterizing FRPs' delamination resistance under transverse loading has long been a major task for many materials engineers and scientists.

Common approaches to characterizing the delamination resistance are based on either load (Ref 4-6) or energy criteria (Ref 7-9). The latter has the advantage of being able to correlate the delamination resistance with the interlaminar fracture toughness and thus is not subject to dimension restrictions. However, at present, the energy criterion is far from ideal for practical use due to the lack of information on the fraction of the total energy loss used for delamination.

The most detailed study reported so far to partition the energy loss was conducted by Delfosse and Poursartip, who considered two mechanisms for damage development in carbon-fiber-reinforced polymers (CFRP) (Ref 9). The mechanisms are (a) delamination and the associated matrix cracking and (b) fiber breakage. Energy loss for contact indentation was considered but was found to be insignificant for the CFRP. However, the study did not consider the energy loss due to friction between delaminating surfaces, which, as suggested later by Symons, should have been considered as an attribute to the energy (Ref 10).

This paper reports a study that took an approach similar to that by Delfosse and Poursartip but on glass-fiber-reinforced polymers (GFRPs). The GFRP is known to have fiber breakage occur at a much later stage than delamination; therefore, the fiber breakage can be excluded by limiting the maximum level of the transverse loading. This reduces the amount of total energy loss and improves the measurement accuracy of the energy loss for the remaining three mechanisms, namely, (a) contact indentation, (b) friction between delaminating surfaces, and (c) matrix cracking and delamination. By measuring the energy loss for items (a) and (b), and subtracting it from the total energy loss, the energy loss for item (c) can be determined. This paper uses this approach to determine how the total energy loss is divided among the three mechanisms in a GFRP under the transverse loading.

2. Experimental

2.1 Materials

GFRP plates 220 × 220 mm^2 were fabricated using a wet hand lay-up technique. The GFRP consists of isophthalic polyester (TMR300, provided by Viking Plastics, Edmonton, Alberta, Canada) as the matrix and unidirectional glass fiber fabric of 9-oz/yd^2 (provided by ZCL Composites, Edmonton, Alberta, Canada) as the reinforcement. Nominal thickness of the plates was 6.5 mm and fiber lay-up $[(0/90)_6]_s$. Overall fiber volume fraction was around 44%, estimated based on the following equation (Ref 11):

$$V_f = \frac{FAW \cdot N \cdot 100}{FD \cdot 2h} \quad \text{(Eq 1)}$$

where FAW is the area weight of the fiber fabric (9 oz/yd^2 or 0.3046 kg/m^2), N is the number of fiber layers (equal to 24 in

T. Kuboki, Department of Mechanical Engineering and Department of Civil & Environmental Engineering, University of Alberta, Edmonton, AB, Canada, T6G 2G8; **P-Y.B. Jar,** Department of Mechanical Engineering, University of Alberta, Edmonton, AB, Canada, T6G 2G8; and **J.J.R. Cheng,** Department of Civil & Environmental Engineering, University of Alberta, Edmonton, AB, Canada, T6G 2G7. Contact e-mail: tkuboki@ualberta.ca.

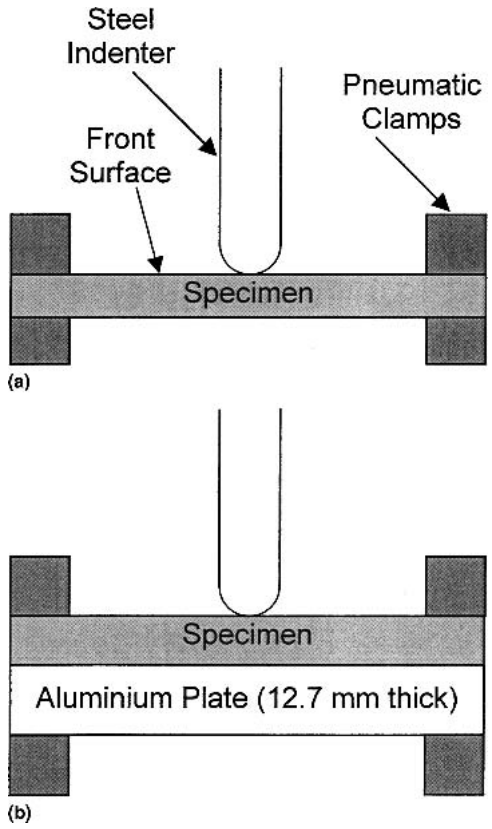

Fig. 1 Schematic diagram of the experimental setup for (a) deflection tests (1st and 2nd) and (b) indentation tests.

this study), *FD* is the fiber density (2560 kg/m^3), and 2*h* is specimen thickness (0.0065 m). The unidirectional glass fiber fabric consists of fiber bundles in the warp direction, separated by a gap of around 1 mm using stitching threads (Ref 12). Due to the gap between the fiber bundles, resin-rich zones exist in the intralaminar, interfiber-bundle regions. GFRP specimens 98 × 98 mm^2 were then machined from the plates for the following mechanical tests.

2.2 Mechanical Tests

Two types of mechanical tests were conducted, both under transverse loading. The first test, called the "deflection test" with the setup shown in Fig. 1(a), was used to measure the total or the frictional energy loss. The second test, called the "indentation test" with the setup shown in Fig. 1(b), was used to measure the energy loss for the indentation damage. Both tests were conducted using an Instron universal testing machine. A pneumatic clamp device with a central circular hole 76.2 mm in diameter, provided by Instron (Instron Corporation, Canton, MA), was used to clamp the specimen for the testing. Preliminary tests were conducted to determine the pneumatic pressure required to firmly clamp the specimen without any slippage during the test. As a result, frictional energy loss due to slippage between the specimen and the clamping plates was deemed negligible. Attention was also paid to ensure that the clamping pressure was not excessive so it did not cause compressive damage to the specimen surface.

For the deflection test, load was introduced at the center of the specimen by a cylindrical steel indenter with a hemispherical nose 12.7 mm in diameter. The load was measured using a load-cell connected to the steel indenter, and displacement of the indenter was calculated based on the crosshead speed that was 1.27 mm/min for loading and 12.7 mm/min for unloading. The increased unloading rate was to reduce the possibility of further damage development during the unloading stage. Four loading levels, 3.42, 5.61, 7.35, and 8.85 kN, as marked on the load–displacement curve in Fig. 2, were applied to specimens for the measurement of the energy loss. The maximum load of 8.85 kN was selected because it was sufficient to generate extensive delamination but without tensile fracture of the fiber. The minimum load of 3.42 kN, Point I in Fig. 2, was selected because it was below the critical load for the onset of delamination, which could cause the slope change of the load–displacement curve (Ref 13, 15). The other three loads, including the maximum load of 8.85 kN, were above the critical load.

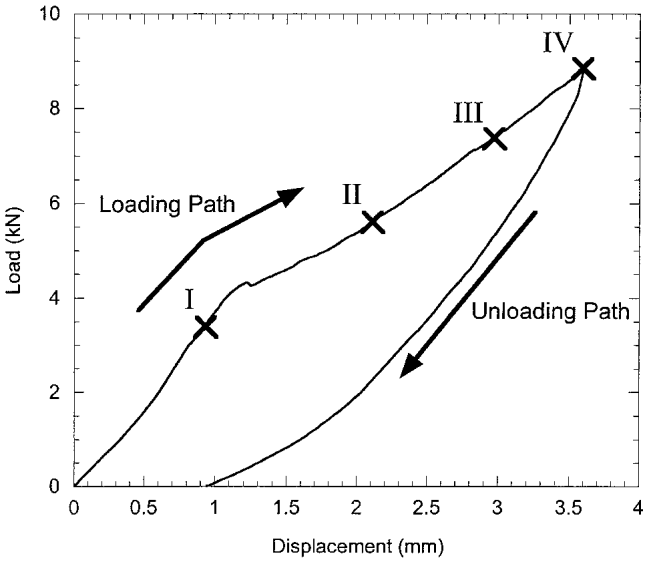

Fig. 2 Typical loading–unloading path of a 1st deflection test, where four points, labeled I to IV, marked the loading levels for the measurement of the energy loss.

The deflection tests for the measurement of frictional energy loss were carried out on the identical specimens that had been loaded to the same level. In other words, each GFRP specimen for the deflection test was subjected to two sequential tests using the identical setup, the first test to initiate the damage and to measure the total energy loss, followed by the second test to measure the frictional energy loss at the same loading level. Caution was taken to prevent the specimens from further delamination during the second test. For clarity, the 2nd deflection test will sometimes be referred to as "friction test."

The indentation tests were carried out on untested specimens using the same 4 loading levels as those for the deflection tests. The setup and loading condition for the indentation test are different from those for the deflection test in two aspects: (a) the indentation test used an aluminium plate, 12.7 mm thick, to provide back support to the specimens and a linear variable differential transformer (LVDT) to measure the displacement of the indenter, and (b) the cross-head speed for the indentation test was 1.27 mm/min for both loading and unloading.

Since the load–displacement curves from the deflection tests (both 1st and 2nd) and the indentation tests were very reproducible, only one specimen was used for each test on a

given loading level. Damage generated by the above mechanical tests was photographed directly under reflected light.

3. Deduction of Energy Loss for Delamination Under Transverse Loading

The approach to quantify the energy loss for each damage mode under the transverse loading is described as follows. The total energy loss of GFRP under transverse loading (E_T) is the difference between input energy (W) and energy stored for the elastic deformation (E_{El}). That is:

$$E_T = W - E_{El} \quad \text{(Eq 2)}$$

In a deflection test, W corresponds to the area under the loading path of the load–displacement curve, and E_{El} corresponds to the area under the unloading path. Therefore, the area enclosed by the loading-unloading curve is equivalent to E_T, as depicted in Fig. 2.

Total energy loss (E_T) is equivalent to the summation of the energy loss due to delamination and the associated matrix cracking (E_{Del}) and that due to the contact indentation (E_{In}). That is:

$$E_T = E_{Del} + E_{In} \quad \text{(Eq 3)}$$

where E_{Del} can be divided into two parts: the energy for the generation of delamination cracks (E_{DelG}) and the frictional energy loss between the delamination surfaces during unloading (E_{DelF}). Therefore, the energy for delamination and matrix cracking (E_{DelG}) can be expressed as:

$$E_{DelG} = E_T - E_{DelF} - E_{In} \quad \text{(Eq 4)}$$

The energy loss due to the contact indentation (E_{In}) can be determined from the indentation tests. Similarly, the frictional energy loss (E_{DelF}) can be determined from the area under the load–displacement curve in the friction test (E_F). Since E_{DelF} is the frictional energy loss between the delamination surfaces during the unloading process, while E_F is the frictional energy loss during both loading and unloading processes, it is reasonable to assume that:

$$E_{DelF} = \frac{E_F}{2} \quad \text{(Eq 5)}$$

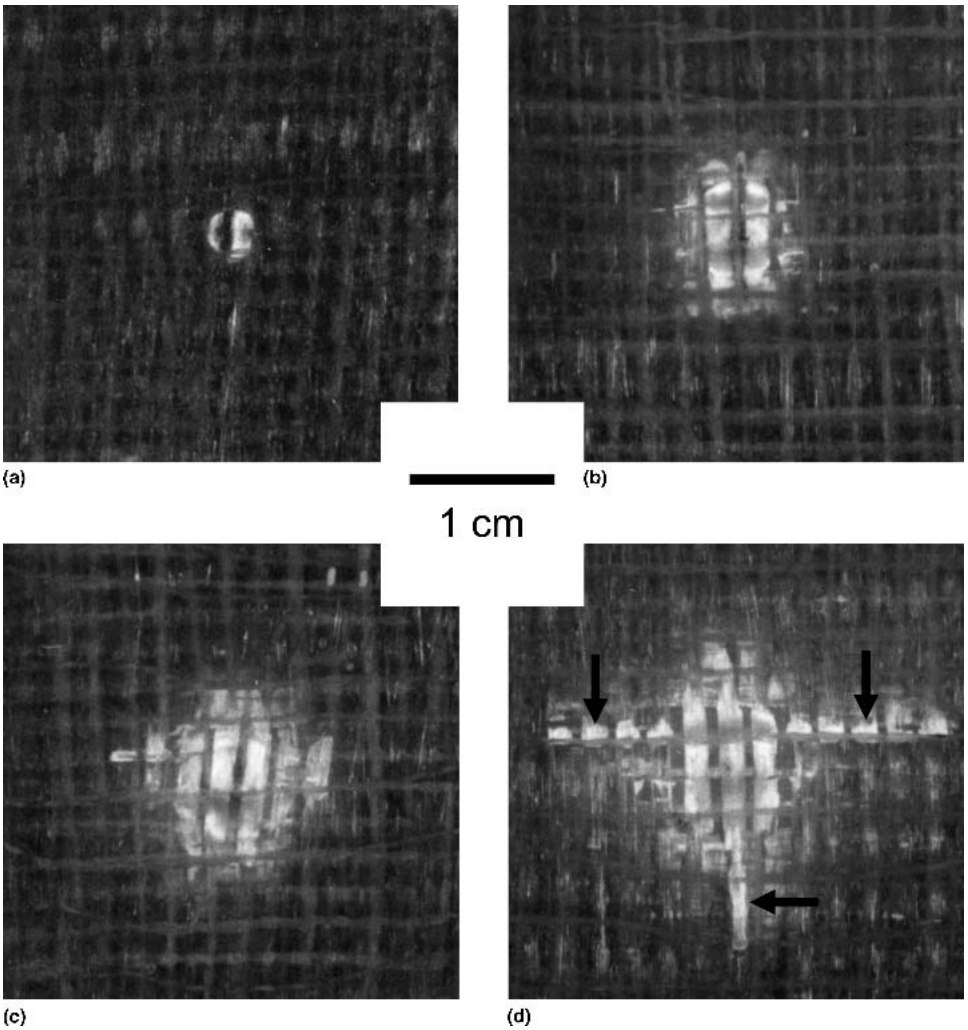

Fig. 3 Optical photographs of damages from the deflection test, viewed on the specimen contact surface at the loading levels of (a) 3.42 kN, (b) 5.61 kN, (c) 7.35 kN, and (d) 8.85 kN (as marked by I to IV in Fig. 2, respectively). Arrows in (d) indicate the fiber buckling.

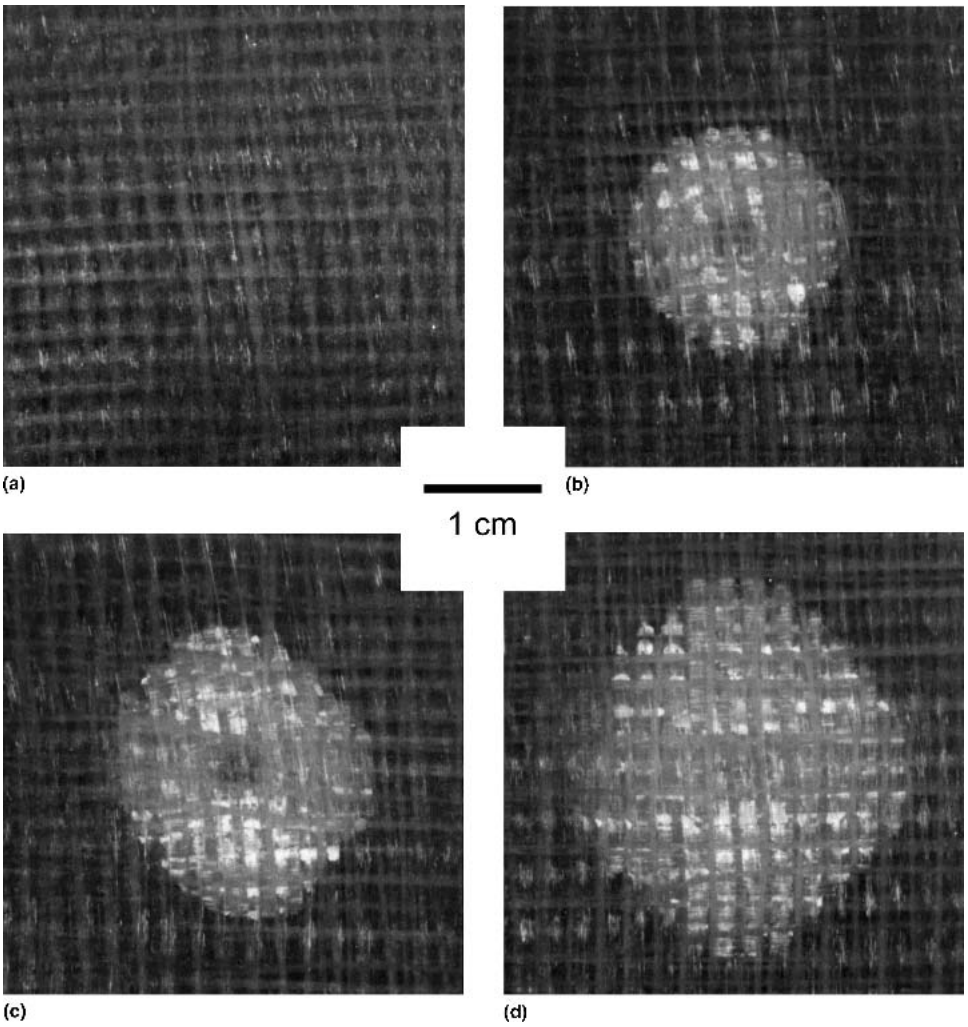

Fig. 4 Optical photographs of back surface of specimens loaded to (a) 3.42 kN, (b) 5.61 kN, (c) 7.35 kN, and (d) 8.85 kN in the deflection tests (as marked by I to IV in Fig. 2, respectively).

4. Results and Discussion

Typical damage patterns from the two deflection tests, viewed on the contact surface, are shown in Fig. 3. The damage pattern in Fig. 3(a), generated by a load of 3.42 kN, is the smallest damage that could possibly be detected by the naked eye. Since the load–displacement curve at this loading level did not show any change of the slope, as shown in Fig. 2, the damage must have been limited to the immediate region around the contact point.

Further increase of the load to 5.61 and 7.35 kN enlarged the size of the contact indentation damage, as shown in Fig. 3(b) and (c). When the maximum load of 8.85 kN was used, some fiber in the surface layer contacting with the indenter fractured in a buckling mode, as shown by arrows in Fig. 3(d).

Damage patterns appearing on the other side of the specimens for Fig. 3 (named back surface) are shown in Fig. 4. Figure 4(a), from the specimen under the load of 3.42 kN, does not show any visible damage. However, bending cracks that are known to start in a very early stage of loading must have been generated on the back surface (Ref 14). These bending cracks, however, are not visible simply due to their low contrast with the surrounding matrix.

When the maximum load was increased to beyond the critical load for the slope change in the loading path of Fig. 2, a circular delamination region can be seen from the back surface, as shown in Fig. 4(b). The size of the delamination was further enlarged by the increase of the load and eventually formed a rhomboid shape, as shown in Fig. 4(c) and (d). The process of the damage development induced by the transverse loading, as shown in Fig. 3 and 4, indicates that the contact indentation was initiated earlier than the delamination, and that both types of damage grew with the increase of the applied load.

Figure 5 presents the typical load–displacement curves from the deflection tests that generated the damages shown in Fig. 3 and 4, and Fig. 6 presents those from the indentation test under the same loading levels. In Fig. 5, the dashed lines represent the 1st deflection tests for the measurement of the total energy loss (E_T) and the solid lines the second deflection tests for the measurement of the frictional energy loss (E_F). Displacement was measured with respect to the original point of contact on the specimen surface. Therefore, the second deflection test started at a displacement that was equivalent to the final displacement from the 1st deflection test. As expected, a slope drop occurred in the 1st deflection tests in Fig. 5(b)-(d), sug-

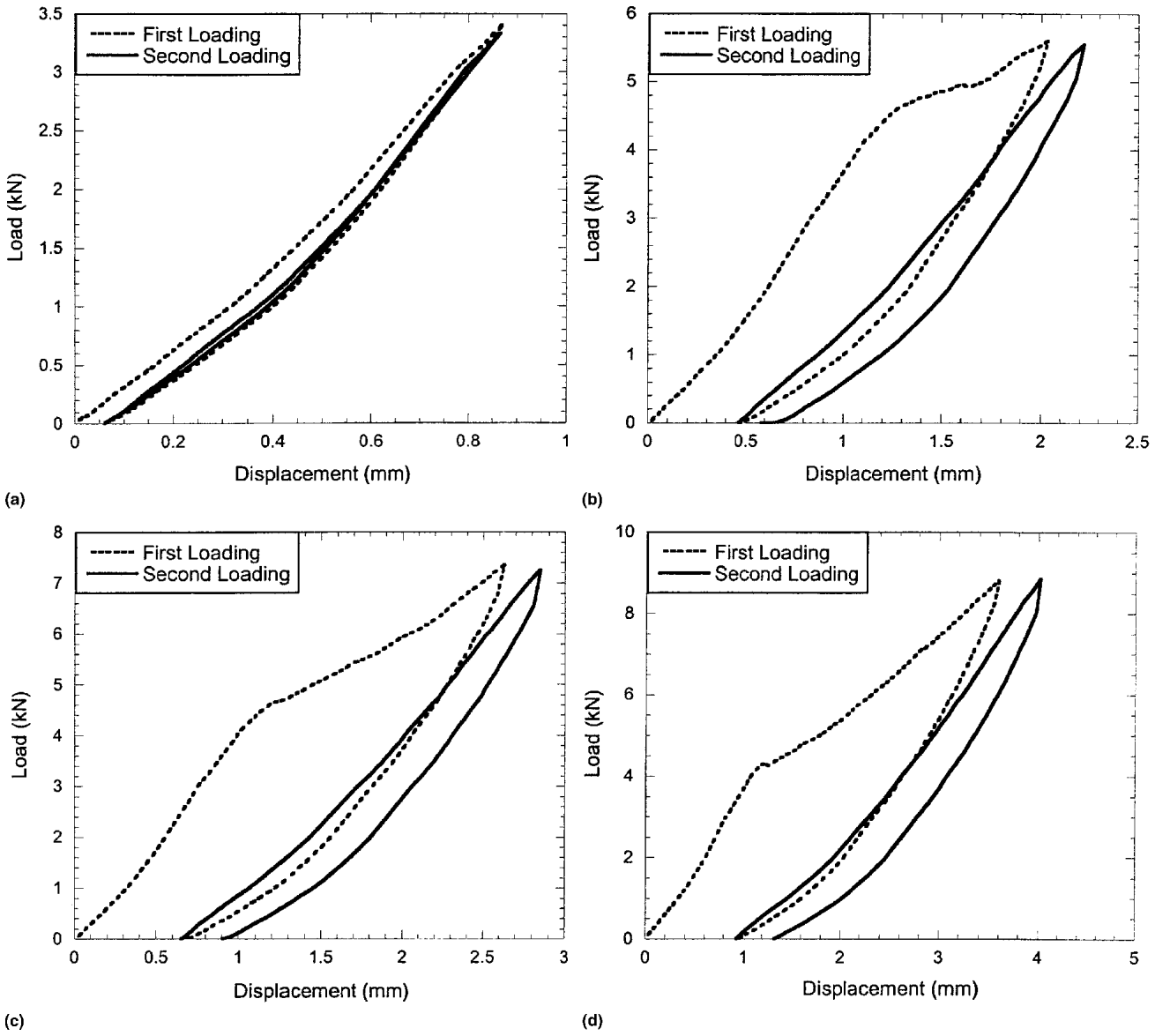

Fig. 5 Typical load–displacement curves of specimens from the first (dotted line) and the second (solid line) deflection tests, with the loading levels at (a) 3.42 kN, (b) 5.61 kN, (c) 7.35 kN, and (d) 8.85 kN (as marked by I to IV in Fig. 2, respectively).

gesting that delamination occurred in these specimens, which is consistent with the photographs presented in Fig. 4.

As mentioned earlier, the total energy loss (E_T), the frictional energy loss (E_{DelF}), and the energy loss for contact indentation (E_{In}) correspond to the area enclosed by the load–displacement curves from the 1st deflection test of Fig. 5, half of the area from the second deflection test of Fig. 5, and the area from the corresponding indentation test of Fig. 6, respectively. The energy loss due to delamination and the associated matrix cracking can then be calculated based on Eq 4 and 5, and the results are summarized in Fig. 7. A vertical dotted line is positioned in both figures of Fig. 7 at the loading level at which the stiffness drop occurred in the first deflection test. Figure 7(a) presents the absolute values of the energy loss as a function of the applied load, and suggests that at the loading level of 3.42 kN, E_T is very small, nearly equal to E_{In}, with E_{DelF} close to zero. When the load exceeded the critical loading level for the stiffness drop (E_T), E_{DelG}, and E_{DelF} increased significantly, compared with the increase of E_{In}. Since the stiffness drop was an indication of delamination, the dramatic increase of E_{DelG} and E_{DelF} must have been caused by the formation of delamination cracks. Further increase of the applied load to the levels of 7.35 and 8.85 kN has increased all types of energy loss in an approximately linear fashion.

It should be noted that E_{DelG} includes the energy loss for delamination and that for matrix cracking. Our earlier study has shown that the formation of matrix shear cracks mingles with that of delamination, making it very difficult to further partition the energy loss E_{DelG} into those for delamination and for matrix shear cracking (Ref 14).

Values of E_{DelF}, E_{In}, and E_{DelG} are presented in Fig. 7(b) as a fraction of the corresponding E_T. As shown in Fig. 7(b), when loaded above the critical loading level, each of the energy absorption modes showed the energy loss as a nearly constant fraction of E_T. The figure indicates that once the delamination occurs, the frictional energy loss (E_{DelF}) takes approximately 20% of the total energy loss. The energy loss for contact indentation (E_{In}) takes another 10% of the total energy loss.

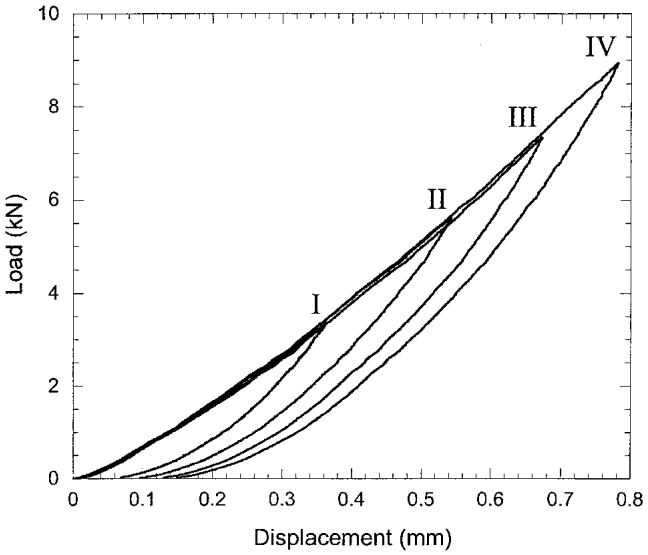

Fig. 6 Typical load–displacement curves from the indentation tests where curves I to IV were obtained from the loading levels of 3.42, 5.61, 7.35, and 8.85 kN, respectively.

Therefore, delamination and the associated matrix cracking (E_{DelG}) consumed only about 70% of the total energy loss.

In principle, the formation of bending cracks should also have contributed to the total energy loss. However, this study has found that the fraction of the total energy loss for generation of bending cracks is negligible, especially after the delamination occurred.

5. Conclusions

Energy loss for contact indentation, delamination and the associated matrix cracking, and friction between delaminating cracks was partitioned in terms of the total energy loss under transverse loading. The results showed that approximately 20% of the total energy loss was consumed by the frictional energy loss, another 10% for the contact indentation, and only the remaining 70% of the total energy loss was used for the delamination and the corresponding matrix cracking. Therefore, any attempt to correlate the impact resistance of the GFRP with its delamination resistance needs to exclude the energy loss for the friction and the contact indentation from the total energy loss. Otherwise, the delamination toughness based on the energy criterion would overestimate the true toughness of the GFRP when subject to transverse loading.

Since load–displacement curves from low-speed impact are very similar to those from the quasi-static loading (Ref 14), conclusions drawn from this study are expected to be applicable to the GFRP when subjected to low-speed impact.

Acknowledgments

The work was sponsored by Intelligent Sensing for Innovative Structures (ISIS) Canada and the Natural Sciences and Engineering Research Council of Canada (NSERC). We are grateful to B. Faulkner and A. Yuen in the Department of Mechanical Engineering, University of Alberta for the technical assistance.

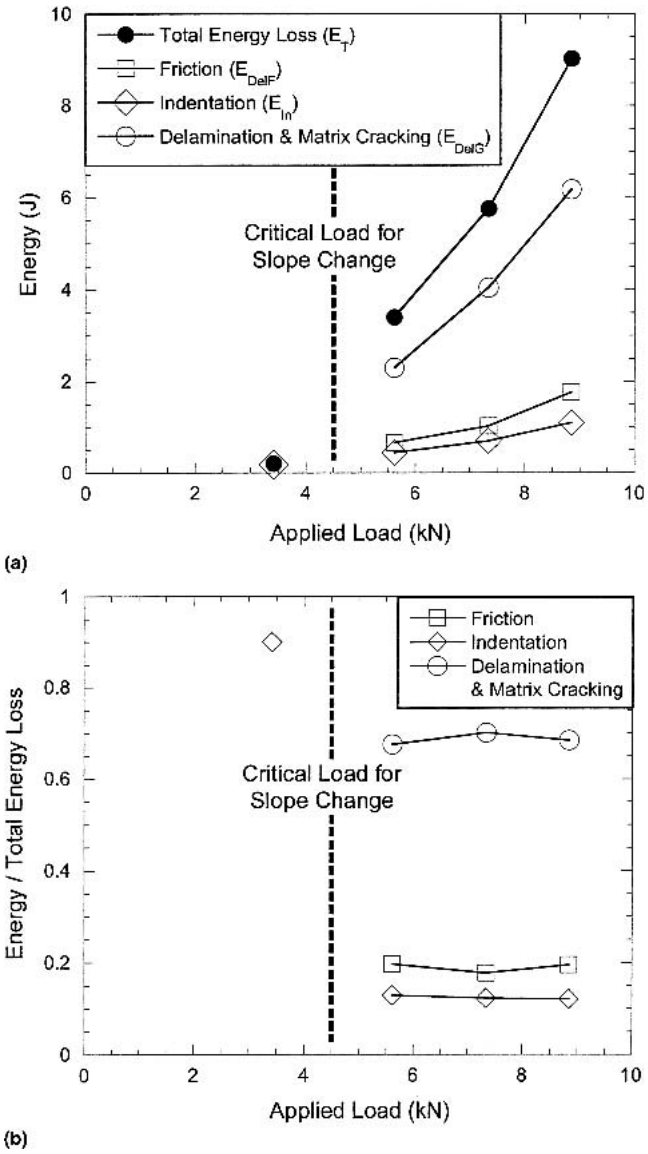

Fig. 7 Partitioning of energy loss in the first deflection tests: (a) absolute energy loss and (b) energy loss as a fraction of the total energy loss for each mode of energy absorption as a function of the applied load.

References

1. S. Abrate, Impact on Laminated Composite Materials, *Appl. Mech. Rev.,* Vol 44, 1991, p 155-190
2. S. Abrate, Impact on Laminated Composites: Recent Advances, *Appl. Mech. Rev.,* Vol 47, 1994, p 517-544
3. M.O.W. Richardson and M.J. Wisheart, Review of Low-Velocity Impact Properties of Composite Materials, *Composites Part A,* Vol 27A, 1996, p 1123-1131
4. C.C.Jr. Poe, Relevance of Impacter Shape to Nonvisible Damage and Residual Tensile Strength of a Thick Graphite/Epoxy Laminate, in *Composite Materials: Fatigue and Fracture,* Vol 3, ASTM STP 1110, T.K. O'Brien, Ed., American Society for Testing and Materials, Philadelphia, 1991, p 501-527
5. W.C. Jackson and C.C.Jr. Poe, The Use of Impact Force as a Scale Parameter For the Impact Response of Composite Laminates, *J. Comp. Tech. Research.,* Vol 15, 1993, p 282-289
6. P.A. Lagace, J.E. Williamson, P.H.W. Tsang, E. Wolf, and S.A. Thomas, A Preliminary Proposition for a Test Method to Measure (Impact) Damage Resistance, *J. Rein. Plast. Comp.,* Vol 12, 1993, p 584-601

7. L.E. Doxsee, P. Rubbrecht, L. Li, I. Verpoest, and M. Scholle, Delamination Growth in Composite Plates Subjected to Transverse Loads, *J. Comp. Mater.,* Vol 27, 1993, p 764-781
8. R.H. Zee and C.Y. Hsieh, Energy Loss Partitioning during Ballistic Impact of Polymer Composites, *Polym. Compos.,* Vol 14, 1993, p 265-271
9. D. Delfosse and A. Poursartip, Energy-based approach to impact damage in CFRP laminates, *Composites Part A,* Vol 28A, 1997, p 647-655
10. D.D. Symons, Characterization of Indentation Damage in 0/90 lay-up T300/914 CFRP, *Compos. Sci. Tech.,* Vol 60, 2000, p 391-403
11. Protocols for Interlaminar Fracture Testing of Composites, European Structural Integrity Society (ESIS), Delft, The Netherlands, 1993
12. T. Kuboki, T. Hilvo, and P.Y.B. Jar, Detection of Interlaminar Cracks in Fibre-Reinforced Polymers (FRP), *J. Mater. Sci. Lett.,* Vol 21, 2002, p 1789-1791
13. M. Davallo, M.L. Clemens, H. Taylor, and A.N. Wilkinson, Low Energy Impact Behaviour of Polyester-Glass Composites Formed by Resin Transfer Moulding, *Plastics, Rubber and Composites Processing and Applications,* Vol 27, 1998, p 384-391
14. T. Kuboki, P.Y.B. Jar, and J.J.R. Cheng, Damage Development in Glass Fiber Reinforced Polymers (GFRP) under Transverse Loading, in *Proceedings of Annual Technical Conference 2003 of Society of Plastics Engineers,* Nashville, TN, The Society of Plastics Engineers, 2003, p 2168-2172